Desalination and Water Treatment
www.deswater.com

doi: 10.1080/19443994.2015.1062429

57 (2016) 14290–14303
June

Taylor & Francis
Taylor & Francis Group

Removal of chromate from aqueous solutions by dendrimers-clay nanocomposites

Abdellah Beraa[a,b,c], Mohamed Hajjaji[a,*], Régis Laurent[b,c], Béatrice Delavaux-Nicot[b,c], Anne-Marie Caminade[b,c]

[a]*Laboratoire de Physico-chimie des Matériaux et Environnement, Unité Associée au CNRST (URAC 20), Faculté des Sciences Semlalia, Université Cadi Ayyad, B.P. 2390, Av. Pce My Abdellah, 40001 Marrakech, Morocco, Tel. +212 67 0233971; email: abdellah.beraa@edu.uca.ma (A. Beraa), Tel. +212 524434649; email: hajjaji@uca.ma (M. Hajjaji)*
[b]*CNRS, LCC (Laboratoire de Chimie de Coordination du CNRS), 205 route de Narbonne, BP 44099, F-31077 Toulouse Cedex 4, France, Tel. +33 753948398; emails: regis.laurent@lcc-toulouse.fr (R. Laurent), beatrice.delavaux-nicot@lcc-toulouse.fr (B. Delavaux-Nicot), caminade@lcc-toulouse.fr (A.-M. Caminade)*
[c]*Université de Toulouse, UPS, INPT, F-31077 Toulouse Cedex 4, France*

Received 28 November 2014; Accepted 7 June 2015

ABSTRACT

Nanocomposites of phosphorus-based dendrimers and montmorillonite were prepared and examined using X-ray diffraction, thermal analysis, solid-state nuclear magnetic resonance, and high-resolution transmission electron microscope. The adsorption of chromate by the nanocomposites and the basic clay was studied in the temperature range 298–318 K. For the latter purpose, the kinetics was followed and adsorption isotherms were plotted. The results showed that intercalated nanocomposites (GC1-AT) were formed with the first generation of cationic dendrimers. The use of the second generation of cationic dendrimers resulted in the formation of a mixture of exfoliated and intercalated nanocomposites (GC2-AT). For both dendrimers, adsorption was by cation exchange. The kinetics of the adsorption of chromate on both nanocomposites and Na-saturated montmorillonite (Na-AT) followed the pseudo-second-order equation and the rate constants varied in 0.08–0.19 g/mmol s^{-1}. The rate-limiting steps were discussed on the basis of the results of the external mass transfer and the internal diffusion models. The experimental isotherms fitted will the model of Temkin, and chromate adsorption was an endothermic process and occurred spontaneously ($-13 < \Delta G^{\circ} < -6$ kJ/mol). The maximum uptake amounts of chromate were in the range 23–38 mg/g. It was shown that as a result of the adsorption of chromate by Na-AT, the adjacent environment of the tetrahedral sheet cation (Si^{4+}) changed. For GC1-AT, the closest environment of the phosphorus atoms of the confined dendrimers was modified, and the interlayer expanded. In the case of GC2-AT, both environments of Si^{4+} and the inner phosphorus atom of the dendrimers became shielded and the interlayer shrunk.

Keywords: Nanocomposites; Dendrimers; Clay; Adsorption; Chromate

*Corresponding author.

1. Introduction

Among the five main families of nanocomposites defined by Komarneni [1], the intercalation-type nanocomposites aroused enormous interest, mainly driven by polymer–clay nanocomposites (PCN). Improvements in the mechanical and thermal properties of PCN, compared with pristine materials, led to industrial uses for more than 25 years [2].

Because of their lamellar structure and their high specific surface area (up to 750 m^2/g) and cation-exchange capacity (up to 1.5 meq/g), smectite clay minerals retained cationic chemical species and various organic polymers [3,4]. In the latter case, nanocomposites with exfoliated or intercalated configurations, or microcomposites, may be formed [5–7].

Clay-based nanocomposites involving pseudo-linear or simple branched polymers were extensively investigated, but only a little attention has been paid to clay nanocomposites with dendrimers. One can cite mainly the interaction of hydrotalcite with polyamidoamine dendrimers [8], of montmorillonite with dendrimers [9], and of polyester dendrimers with clays, which led to original moldable hydrogels [10].

Cr(VI)-based salts are commonly used in leather manufacturing and surface treatment of metals. Effluents from such units of treatment are loaded with Cr(VI), known as a powerful oxidant and hazardous chemical pollutant [11]. Therefore, many studies have been devoted to its removal from aqueous solution using among others low-cost adsorbents [12]. In this respect, it has been reported that the maximum adsorption capacity of Cr(VI) by some modified clay minerals, such as montmorillonite, exceeded those of some activated carbons [13,14].

The aim of this work was to prepare and carry out a chemical and structural characterization of nanocomposites of montmorillonite and phosphorus-based dendrimers with ammonium cations as peripheral ends. Moreover, the process of adsorption of chromate by the prepared nanocomposites and Na-saturated montmorillonite was investigated. For the latter study, the kinetics was followed and adsorption isotherms were measured.

2. Materials and experimental procedures

2.1. Materials

The clay used in this study was from Tassaout (High-Atlas, Morocco), labeled here as AT. It was essentially composed of montmorillonite. Some of the clay characteristics were reported elsewhere [15].

The first (GC1) and second (GC2) generations of cationic phosphorus-based dendrimers (Fig. 1) were prepared by controlled growth of the structure with successive layers of H_2N–N(Me)–P(S)Cl_2 moieties and 4-hydroxybenzaldehyde.

The ammonium groups were directly obtained by reaction of N,N-diethylethylenediamine with the P(S)Cl_2 terminal groups, and the core was derived from hexachlorocyclotriphosphazene [16]. The presence of the peripheral ammonium groups facilitated water solubility of dendrimers [17,18]. The hydrodynamic radii (R_H) of GC1 and GC2 were determined using the dynamic light scattering technique and the following relation:

$$R_H = k_B T / 6\pi\eta_s D \quad (1)$$

where k_B is the Boltzman's constant, T is the operating temperature (298 K), η_s is the viscosity of the medium (tetrahydrofuran; η_s = 0.48 cP), and D is the diffusion coefficient.

The determined R_H of GC1 and GC2 were 1.1 and 1.5 nm, respectively.

2.2. Experimental procedures

Portions of the sieved AT clay (<80 μm) were dispersed in sodium chloride aqueous solutions (1 M). The dispersions were stirred for 24 h at room temperature and centrifuged (4,000 rpm) to isolate the sediments. The sodium loading operation was repeated four times. The Na-saturated clay (Na-AT) was oven dried (105°C).

A weighed portion of the cationic dendrimers (0.5 g) was introduced into 20 mL of warm distilled water (80°C) and stirred for 15 min. The solution of dendrimers was mixed with 10 mL of an aqueous dispersion containing 3.5 g of Na-AT. The mixture of pH 6.3 was stirred for 24 h at room temperature, and then centrifuged to isolate the solid fraction. The moisture of the isolated sediment was removed by freeze-drying.

For kinetics experiments, mixtures composed of 16 mL of an aqueous dispersion of adsorbent (0.5 g/L) and 40 mL of an aqueous solution of K_2CrO_4 (0.04 mmol/L) were kept at constant temperatures (298, 308, and 318 K) and continuously stirred (250 rpm). The pH was maintained constant (pH 4) by adding droplets of a molar solution of HCl or NaOH. Samples of the mixtures were withdrawn at regular times and centrifuged at 4,000 rpm. The concentration of chromate in the supernatant (C_t) was measured with UV–visible spectrometry following the experimental method reported by Basset et al. [19]. The instantaneous amount of the fixed chromate per mass of adsorbent (q_t) was deduced using the relation:

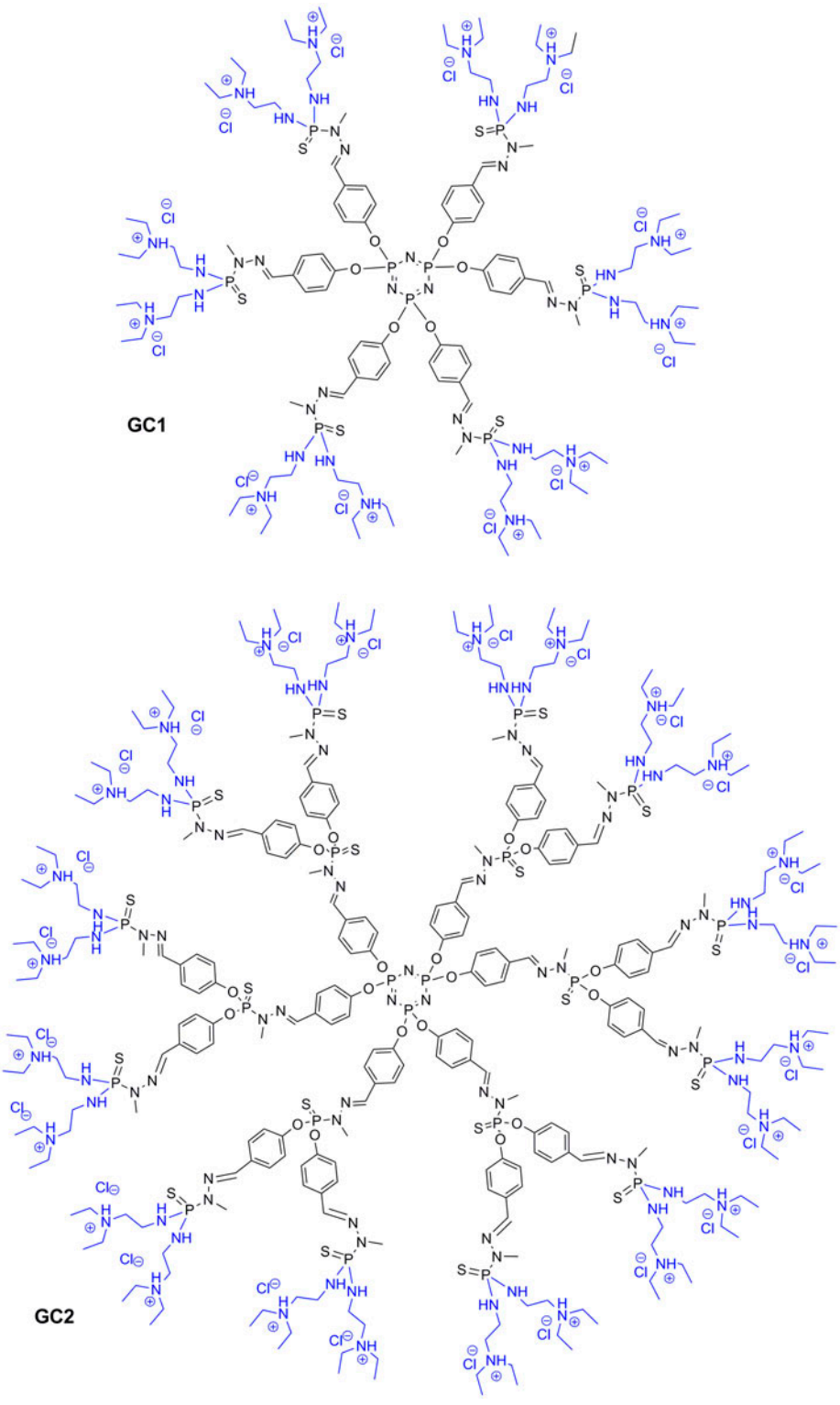

Fig. 1. Schematic representation of the structures of GC1 and GC2 dendrimers.

$$q_t = (C_o - C_t)V/m \quad (2)$$

C_o is the initial concentration; V is the volume of solution; and m is the mass of adsorbent.

Concerning adsorption isotherm measurements, solutions containing each 16 mL of an aqueous solution of adsorbent (0.5 g/L), 40 mL of a solution of chromate (10^{-3}–8×10^{-2} mmol/L), and 24 mL of distilled water were maintained at constant temperatures (298, 308, and 318 K) for 4 h. The solutions were continuously agitated (250 rpm) and their pH was fixed at 4. The uptake amount of chromate was deduced as reported in the above section.

Samples of dried nanocomposites and Na-AT were analyzed with X-ray diffraction (XRD), using an X'Pert-PRO diffractometer operating with a copper anode (K_α = 1.5418 Å). Thermogravimetry (TG) curves were obtained on a SETARAM 92-16.18 apparatus functioning at air atmosphere and 10°C/min. Solid-state nuclear magnetic resonance (NMR) spectra were obtained at ambient temperature on a Bruker Avance 400 WB apparatus. The used frequencies were 8 kHz for ^{31}P, ^{23}Na, and ^{29}Si, and 9 kHz for ^{27}Al. The recycle delays were 2, 3, 10, and 30 s for ^{23}Na, ^{27}Al, ^{31}P, and ^{29}Si respectively. For ^{23}Na analysis, a solution of NaCl (1 M) was taken as a reference. The used references for ^{29}Si, ^{27}Al, and ^{31}P were tetramethylsilane, a diluted aqueous solution of NaCl containing $Al(H_2O)_6^{3+}$ and a phosphoric acid solution (85%), respectively.

High-resolution (HR) examinations of the nanocomposites were carried out with a JEOL JEM 1011 transmission electron microscope (TEM). For this objective, a small drop of a dispersion of the nanocomposite or Na-AT was placed on a copper grid and dried at 35°C for about 20 min.

3. Results and discussion

3.1. Characterization of the prepared nanocomposites

Comparing the XRD patterns of the GC1-AT nanocomposite to that of Na-AT indicated that the nanocomposite had a greater basal spacing (Fig. 2), and therefore GC1 species were intercalated.

In fact, the HR-TEM examinations showed that the structure of the nanocomposite was exclusively composed of packets of layers with basal spacings exceeding 1.34 nm measured for AT (Fig. 3(a)).

As reported elsewhere, the d value from XRD represents the average of the actual basal spacings [20]. Taking into consideration the basal spacing of GC1-AT (1.83 nm) and that of dehydrated montmorillonite (1 nm) [21], the confined GC1 dendrimers lost their original size.

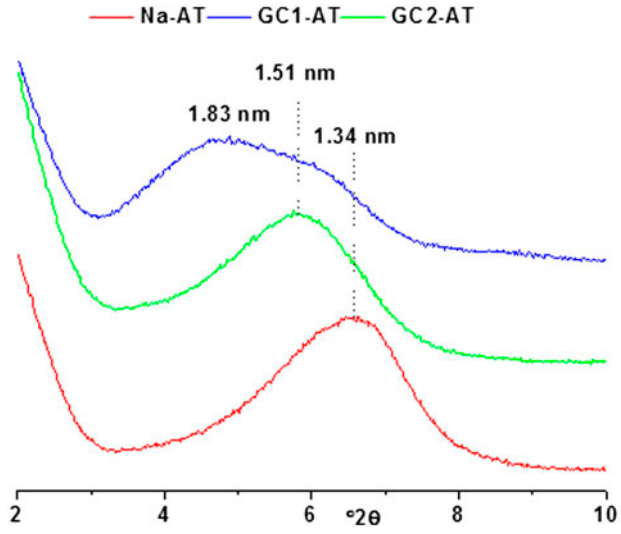

Fig. 2. Sections of the XRD patterns of Na-AT and the prepared nanocomposites.

Referring once again to Fig. 2, the basal spacing (d_{001}) of GC2-AT nanocomposite was somewhat greater than that of Na-AT. Thus, one may wonder whether GC2 dendrimers (1.5 nm radius) entered the interlayer of montmorillonite. The HR-TEM observations of GC2-AT samples revealed ordered layers with different basal spacings together with flat contrast zones (Fig. 3(b)), which were extensively encountered in Na-AT (Fig. 3(c)). Considering the TEM measured spacings, the size of confined GC2 species was reduced by about 75%. By contrast, the size reduction in the case of GC1-AT was 55%.

As a result of the adsorption of dendrimers, the main part of Na^+ ions left the clay structure (Fig. 4). The chemical environment of the remaining Na^+ ions was altered since the chemical shift of ^{23}Na evolved from −5.2 ppm to −13.0 ppm (Fig. 4).

As can be deduced from the TG curves of Fig. 5, losses of physisorbed water occurred at 30–93°C for both nanocomposites and 30–169°C for Na-AT, and their amounts were 2.3, 4.4, and 12.2 wt.% for GC1-AT, GC2-AT, and Na-AT. Thus, the prepared nanocomposites were less hydrophilic. Indeed, the clay hydrophilicity is commonly reduced when inorganic cations are replaced by organic cations [3]. Dendrimers of both nanocomposites were the subject of a first decomposition at 237–295°C and a second at about 670°C. The final decomposition started just as the dehydroxylation process of montmorillonite was completed. Moreover, in the presence of dendrimers, the temperature of dehydroxylation of montmorillonite was enhanced.

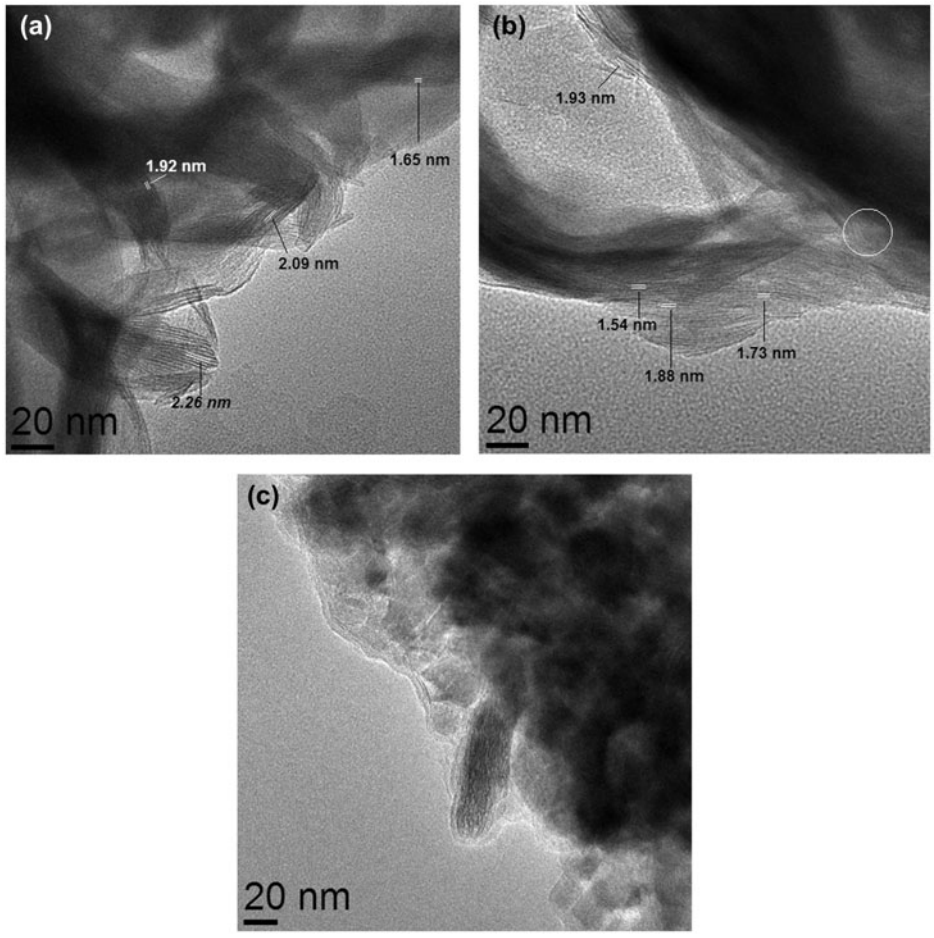

Fig. 3. HR-TEM micrographs of GC1-AT (a), GC2-AT (b), and Na-AT (c).

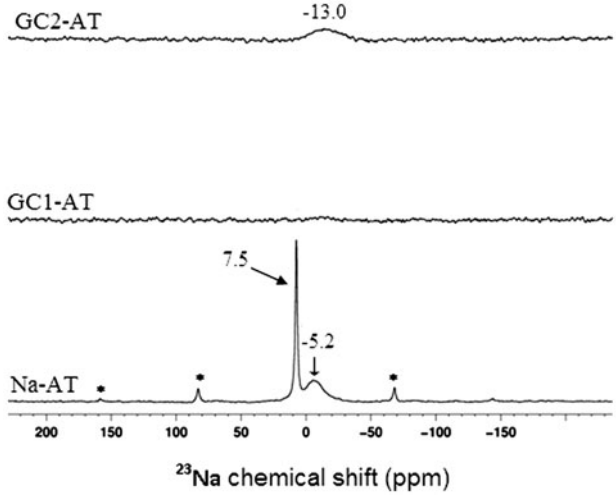

Fig. 4. ^{23}Na solid-state NMR spectra of Na-AT, GC1-AT, and GC2-AT.

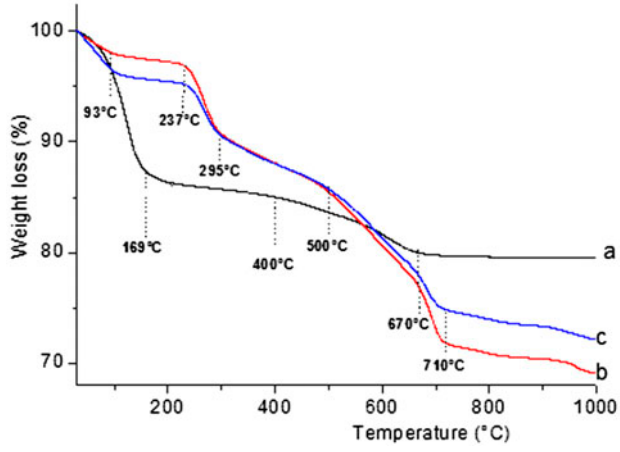

Fig. 5. Thermal curves (TG) of Na-AT (a), GC1-AT (b), and GC2-AT (c) samples.

The results of ^{31}P solid-state NMR of the nanocomposites indicated that the chemical environment of phosphorus was not altered (Fig. 6). The NMR results (Fig. 7) also showed that adsorption of dendrimers did not affect the chemical environment of the octahedral ($\delta(Al^{VI})$ = 4.20 ppm) and tetrahedral ($\delta(Al^{IV})$ = 68.0 ppm) aluminum of montmorillonite [22,23]. Moreover, the chemical environment of the structural silicon ($\delta(Si^{IV})$ = −93.12 ppm) (Fig. 8) was not disturbed.

3.2. Adsorption of chromate on the prepared nanocomposites and Na-saturated montmorillonite

3.2.1. Kinetics study

The kinetics of the adsorption of chromate by the studied adsorbents reached its limit in less than an hour, and the equilibrium time was somewhat short for GC1-AT (Fig. 9).

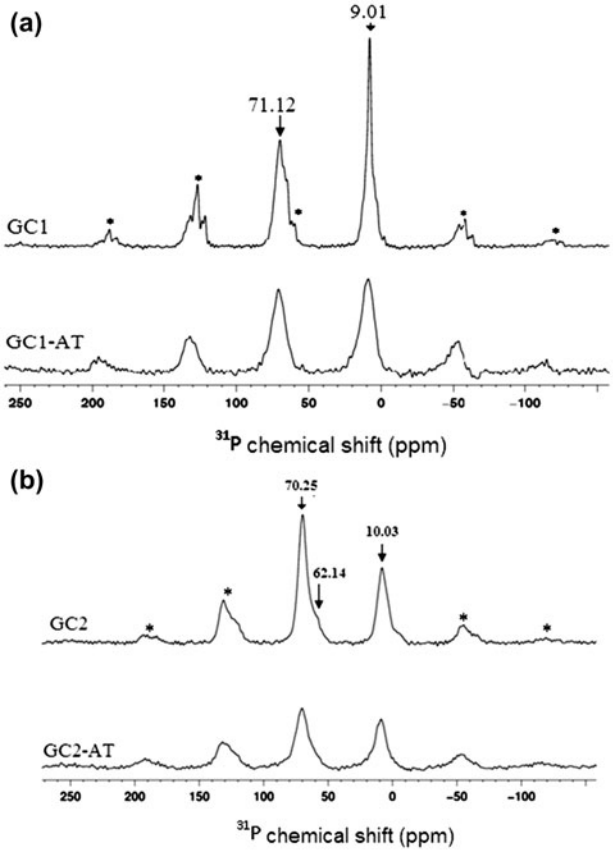

Fig. 6. ^{31}P solid-state NMR spectra of the dendrimers and the prepared nanocomposites. The assignment of bands was based on the data reported by Loup et al. [17]. (*): spinning side bands.

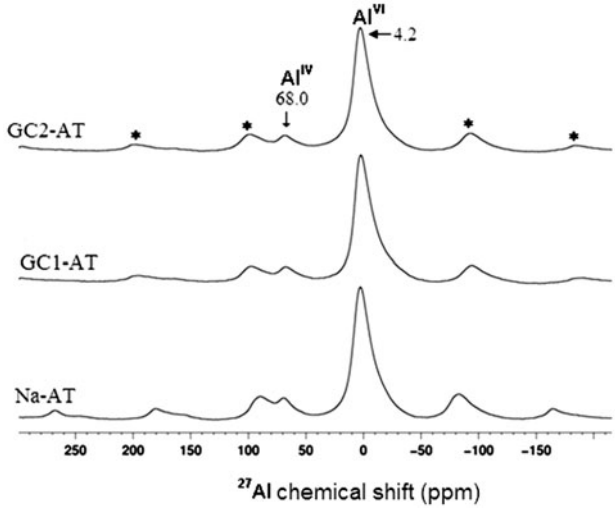

Fig. 7. ^{27}Al Solid-state NMR spectra of Na-AT, GC1-AT, and GC2-AT.

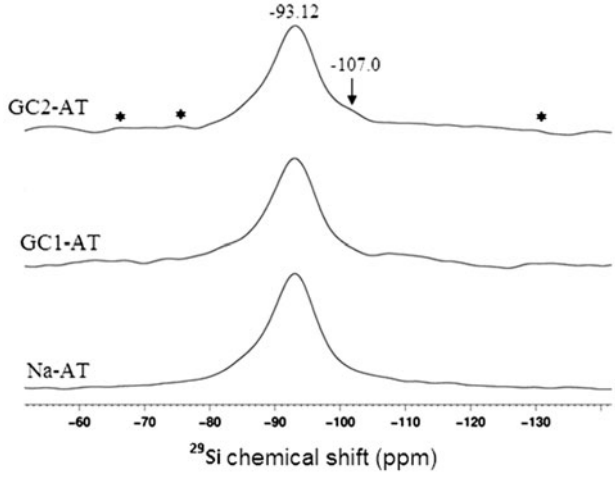

Fig. 8. ^{29}Si solid-state NMR spectra of Na-AT, GC1-AT, and GC2-AT. The shoulder at −107.0 ppm was due to Si of quartz [36].

The kinetics curves fitted better the pseudo-second-order equation:

$$1/(q_e - q_t) = 1/q_e + kt \quad (3)$$

q_e and q_t are the uptake amounts at equilibrium and t instant; k is the rate constant. The values of the fitting coefficients and k are given in Table 1. k varied in the range 0.08–0.19 g/mmol s^{-1} and increased with increasing temperature, except for GC1-AT. The change of the rate constants for Na-AT and GC2-AT against $1/T$ (T: temperature (K)) fairly followed the Arrhenius equation:

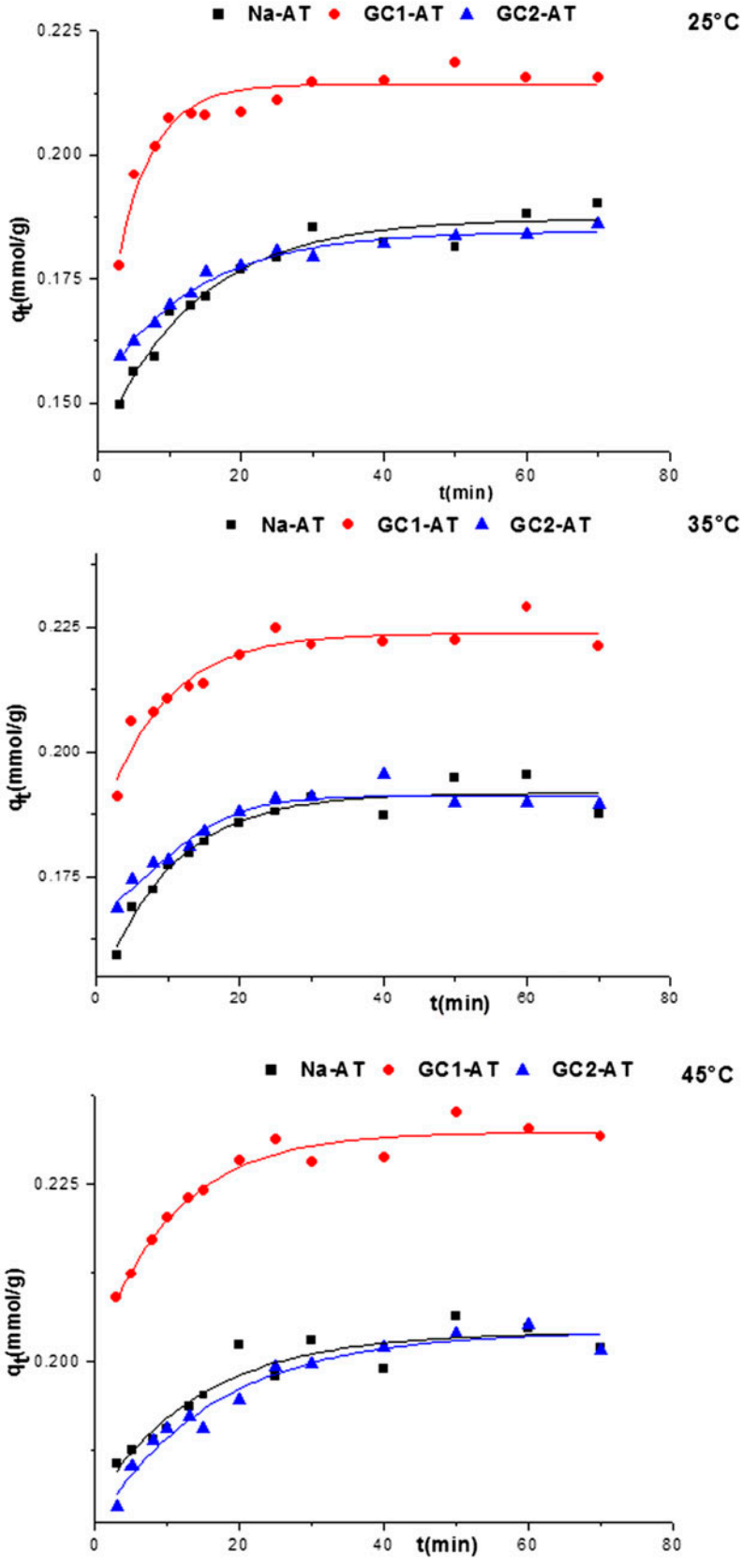

Fig. 9. Curves of the kinetics of chromate adsorption on the studied sorbents plotted at different temperatures.

Table 1
Values of the rate constant (k) and fitting coefficient (R^2) of the pseudo-second-order kinetic equation

		25°C	35°C	45°C
Na-AT	k (g/mmol s^{-1})	8.9×10^{-2}	10.6×10^{-2}	18.5×10^{-2}
	R^2	0.9996	0.9998	0.9996
GC1-AT	k (g/mmol.s^{-1})	14.9×10^{-2}	9.8×10^{-2}	12.3×10^{-2}
	R^2	0.9999	0.9997	0.9998
GC2-AT	k (g/mmol.s^{-1})	11.6×10^{-2}	12.0×10^{-2}	16.7×10^{-2}
	R^2	0.9997	0.9996	0.9997

$$k = A' \exp(-E_a/RT) \quad (4)$$

A' is the frequent factor, E_a, the energy of activation, and R, the gas constant.

The values of E_a were 28 and 114 kJ/mol for Na-AT and GC2-AT, respectively. The Arrhenius equation did not describe properly the result relating to GC1-AT.

To determine the rate-limiting steps, the kinetics data were analyzed with the external mass transfer diffusion model [24]:

$$\ln(C_t/C_o) = -k_f(S/V)t \quad (5)$$

k_f is the external diffusion coefficient (cm/s), S, the external surface area of adsorbent, and V, the volume of solution; $S/V = 110$, 63, and 50 cm^{-1} for Na-AT, GC1-AT, and GC2-AT, respectively. The kinetics data were also analyzed with the internal diffusion model [25]:

$$q_t = k_{ip} t^{0.5} \quad (6)$$

k_{ip} is the intraparticle diffusion constant (mmol/g $s^{-0.5}$).

The following intraparticle mass transfer diffusion model was also used [25]:

$$\ln(1 - F(t)) = -k_{ld} t \quad (7)$$

$F(t) = q_t/q_e$, k_{ld} is the liquid film diffusion constant (s^{-1}).

Taking into consideration the values of the fitting coefficients of Table 2, the rate of adsorption of

Table 2
Values of the constants of the intraparticle (k_{ip}) and the liquid film (k_{ld}) diffusion models and fitting coefficients

		25°C	35°C	45°C
Na-AT	k_{ip} (mmol/g $s^{0.5}$)	1.2×10^{-3}	1.1×10^{-3}	0.6×10^{-3}
	R^2	0.981	0.976	0.936
	C	0.135	0.148	0.177
	k_{ld} (s^{-1})	12.7×10^{-3}	1.7×10^{-3}	1.0×10^{-3}
	R^2	0.990	0.997	0.991
	C'	−1.435	−1.545	−2.297
GC1-AT	k_{ip} (mmol/g $s^{0.5}$)	1.1×10^{-3}	1.2×10^{-3}	0.9×10^{-3}
	R^2	0.853	0.952	0.997
	C	0.174	0.181	0.197
	k_{ld} (s^{-1})	1.4×10^{-3}	1.9×10^{-3}	1.7×10^{-3}
	R^2	0.912	0.968	0.995
	C'	−2.006	−1.768	−1.951
GC2-AT	k_{ip} (mmol/g $s^{0.5}$)	0.9×10^{-3}	0.8×10^{-3}	0.7×10^{-3}
	R^2	0.992	0.993	0.970
	C	0.147	0.158	0.173
	k_{ld} (s^{-1})	1.6×10^{-3}	1.8×10^{-3}	1.1×10^{-3}
	R^2	0.992	0.970	0.963
	C'	−1.624	−1.766	−2.030

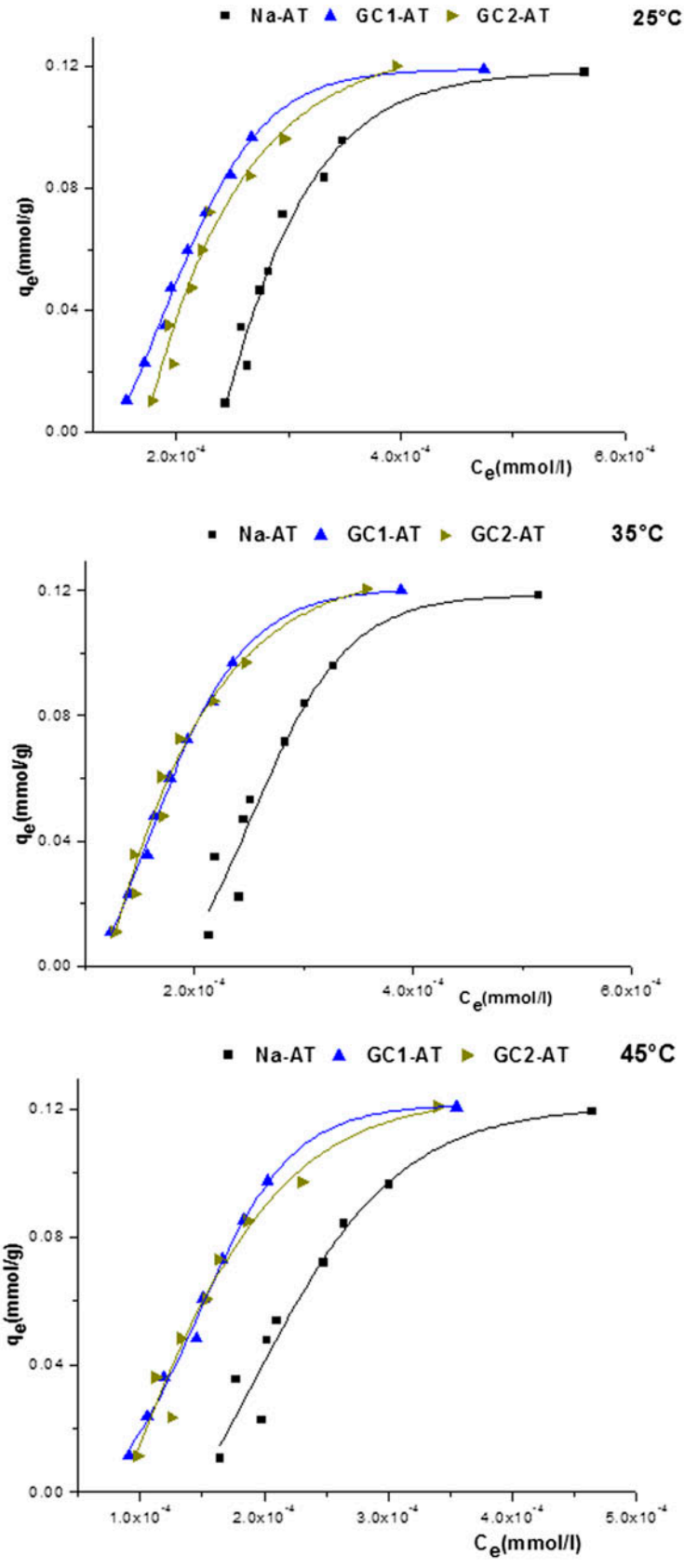

Fig. 10. Adsorption isotherms of Na-AT, GC1-AT, and GC2-AT measured at different temperatures.

Table 3
Parameters of the adsorption isotherm models and values of the correlation coefficients

Model		Na-AT			GC1-AT			GC2-AT		
		25℃	35℃	45℃	25℃	35℃	45℃	25℃	35℃	45℃
L[a]	K_L	<0	<0	<0	<0	<0	<0	<0	<0	<0
	q_m	<0	<0	<0	<0	<0	<0	<0	<0	<0
F[b]	K_F	7,363,162	4,837,942	44.746	524,133	898,067	1.595×10^9	524,133	251,052	47,346,336
	$1/n$	2.333	2.252	0.771	1.927	1.948	2.73562	1.48356	2.06544	2.35013
T[c]	K_T	*4,358*	*5,211*	*9,258*	*6,757*	*8,586*	*6,509*	*6,509*	*9,437*	*12,464*
	B_1	*0.237*	*0.188*	*0.086*	*0.165*	*0.138*	*0.115*	*0.115*	*0.109*	*0.090*
D-R[d]	E	Ind	Ind	Ind	Ind	Ind	Ind	Ind	Ind	Ind
	q_m	3.029×10^8	653.3	7.015	790,167	277.7	28.716	28.716	446.5	106.4
H-J[e]	A	7.257×10^{-5}	7.832×10^{-5}	1.072×10^{-3}	9.407×10^{-5}	9.507×10^{-5}	1.125×10^{-4}	4.148×10^{-5}	9.15×10^{-5}	1.140×10^{-4}
	B´	−3.387	−3.429	−3.335	−3.513	−3.596	−3.662	−3.355	−3.605	−3.650
R^2										
L[a]		0.397	0.421	0.081	0.414	0.478	0.458	0.273	0.506	0.457
F[b]		0.742	0.773	0.745	0.816	0.865	0.979	0.762	0.862	0.901
T[c]		0.971	0.953	0.970	0.996	0.995	0.973	0.928	0.968	0.969
D-R[d]		0.882	0.782	0.939	0.959	0.876	0.910	0.772	0.870	0.878
H-J[e]		0.422	0.453	0.833	0.523	0.580	0.625	0.411	0.562	0.582

Note: Ind: Indeterminate value.
[a]L: $q_e = K_L C_e q_m/(1 + K_L C_e)$.
[b]F: $q_e = K_F(C_e)^{1/n}$.
[c]T: $q_e = (RT/b)\ \ln(K_T C_e)$.
[d]D-R: $q_e = q_m \exp(-Be^2)$.
[e]H-J: $q_e = (B´/A - (1/A)\log C_e)^{-1/2}$.

chromate was mainly limited by internal diffusion. In this respect, it should be noted that the curves $q_t = f(t^{0.5})$ did not go through the origin ($C \neq 0$) and the value of the intercept increased with the increasing temperature (Table 2). This value increase was considered as an indication of the growth of the boundary layer thickness linked to the solute sorption at the boundary layer.

The results of the external mass transfer diffusion model showed that k_f of the process of adsorption of chromate on Na-AT and GC2-AT slightly increased with increasing temperature ($3.7–5.7 \times 10^{-5}$ cm/s for Na-AT and $9.5–11.7 \times 10^{-5}$ cm/s for GC2-AT). The higher value of k_f (14.2×10^{-5} cm/s) for GC1-AT was obtained at the intermediate operating temperature (308 K). In view of these values, the clay modification using GC1 and GC2 dendrimers did not have an appreciable effect on chromate transfer from solution to the surface of particles.

3.2.2. Isotherm measurement and mechanism of adsorption

The experimental isotherms of Fig. 10 were analyzed with different known adsorption isotherm models [15], and the results showed that the Temkin model fairly described the measured isotherms (Table 3). Consequently, chromate adsorption seemed to occur by chemisorption [26].

Considering K_e, the constant expressing the law of mass action of the following equilibrium: $(\text{Chromate})_{\text{solution}} \leftrightarrows (\text{Chromate})_{\text{fixed}}$

$$K_e = a_f/a_s \tag{8}$$

a_f and a_s are the equilibrium activities of chromate in solution and fixed to adsorbent particles.

For dilute solutions, the activities of the chemical species could be replaced by their concentrations (C_i), and therefore:

$$K_e = C_f/C_s \tag{9}$$

where $C_f = q_e$ and $C_s = C_e$.

The value of K_e was taken as the intercept of the linear curve of $q_e/C_e = f(q_e)$ ($q_e \to 0$ for very dilute solution). The determination of K_e was used to calculate the Gibbs free energy:

$$\Delta G_T^\circ = -RT \ln K_e \tag{10}$$

R kept the same meaning.

The change of ΔG_T° against temperature is shown in Fig. 11. It should be noted that $\Delta G_T^\circ < 0$ in the investigated range of temperature. So, chromate was spontaneously adsorbed on the studied adsorbents. The heat (ΔH°) and entropy (ΔS°) of the adsorption process were determined (Table 4) basing on the plot of Fig. 11 and the relation:

$$\Delta G_T^\circ = \Delta H_T^\circ = T\Delta S_T^\circ \tag{11}$$

Chromate adsorption was an endothermic process and took place by chemisorption, particularly for Na-AT and GC2-AT since $\Delta H^\circ > 40$ kJ/mol [27]. This result was in line with the result derived from the isotherm measurements. Considering the entropy values, disorder increased with chromate adsorption.

The maximum uptake amounts of chromate (q_m) were calculated using the relation:

$$q_m = C_o^m/(m/V + 1/K_e) \tag{12}$$

m, V, and K_e kept the same meaning; C_o^m is the maximum concentration of chromate used (8×10^{-2} mmol/L). This relation is the combination of

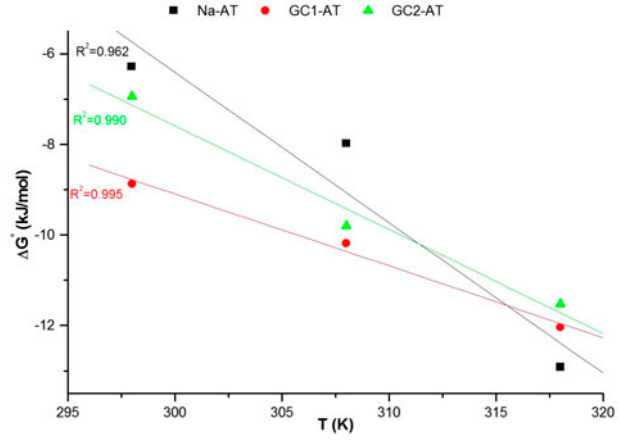

Fig. 11. Variation of the Gibbs free energy of chromate adsorption on the studied sorbents against temperature.

Table 4
Heat and entropy of the adsorption of chromate on the studied sorbents

	ΔH° (kJ/mol)	ΔS° (kJ $K^{-1}mol^{-1}$)
Na-AT	93.116	0.332
GC1-AT	38.484	0.159
GC2-AT	61.124	0.229

Table 5
Maximum amounts of Cr^{VI} retained by some clays, clay-based materials, and the studied adsorbents

Adsorbents	q_m (mg g^{-1})	Refs.
Kaolinite clay	1.51	[28]
Spent activated clay	0.957	[29]
Montmorillonite modified with hydroxyaluminum and cetyltrimethylammomium bromide	11.97	[30]
Bentonite	0.57	[31]
Al-cetyltrimethylammonium bromide-montmorillonite	11.85	[32]
Natural bentonite (Algeria)	12.61	[33]
Hexadecyltrimethyl ammonium-montmorillonite	7.28	[34]
Clay of Jebel M'rhila (Tunisia)	10.9	[35]
Na-montmorillonite	6.2	Present study
GC1-montmorillonite	10.2	
GC2-montmorillonite	7.15	

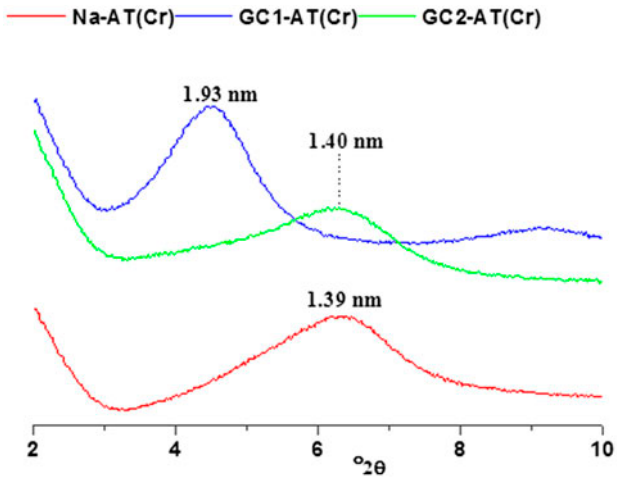

Fig. 12. Sections of the X-ray diffractograms of Na-AT, GC1-AT, and GC2-AT samples, which were in contact with chromate.

Eqs. (2) and (9). The maximum retained amount of chromate varied in the range 23–38 mg/g. At 298 K, q_m for GC1-AT exceeded those calculated for Na-AT and GC2-AT by about 40%. At the high operating temperature, q_m was almost constant (37 mg/g). The maximum retained amounts of Cr^{VI} were greater than those determined for some clays or clay-based adsorbents (Table 5).

As a result of the contact with chromate, the basal spacing of GC1-AT expanded (5%), while that of GC2-AT shrunk (7%) (Fig. 12). In the case of Na-AT, the basal spacing was almost unchanged. For GC2-AT, it seemed that intercalated dendrimers left the interlayer space because its basal distance approached that of Na-AT (Fig. 12).

Chromate adsorption by Na-AT resulted in a negative shift in the ^{29}Si NMR spectra ($\Delta\delta = -2.18$ ppm) (Table 6). Accordingly, the adjacent environment of Si cations (the main species of the tetrahedral sheet of

Table 6
^{27}Al ^{29}Si and ^{31}P NMR chemical shifts of Na-AT. GC1-AT and GC2-AT before and after adsorption of chromate

	Chemical shift (ppm)						Assignments	Refs.
	Na-AT	Na-AT (Cr)	GC1-AT	GC1-AT (Cr)	GC2-AT	GC2-AT (Cr)		
^{27}Al	4.20	4.20	4.20	4.20	4.20	4.20	Al(VI)	[22,23]
	68.00	68.10	68.03	68.10	68.00	68.10	Al(IV)	
^{29}Si	−93.12	−95.30	−93.22	−93.20	−93.05	−93.20	Si(IV)	
	−107.0	−107.0	−107.03	–	−107.02	−107.01	Si (quartz)	[36]
^{31}P			9.01	8.40	10.03	8.90	P0	[17]
			71.12	70.20	62.14	62.40	P1	
					70.25	70.11	P2	

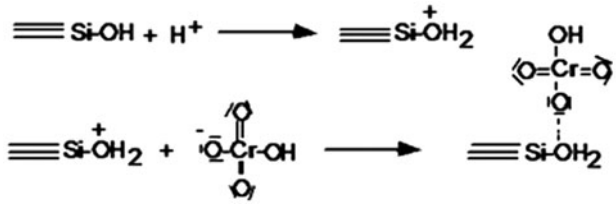

Fig. 13. Schematic representation of the interaction between chromate and montmorillonite.

montmorillonite) became shielded. On the other hand, in the operating acid solutions (pH 4), $HCrO_4^-$ was the most abundant species ($[HCrO_4^-] = 312[CrO_4^{2-}]$). Taking into consideration the above NMR result, $HCrO_4^-$ ions interacted with montmorillonite as depicted in Fig. 13.

The chemical shift of ^{29}Si in GC1-AT remained almost constant after $HCrO_4^-$ fixation (Table 6). So, the above interaction process should be discarded. Due to the adsorption of $HCrO_4^-$ by GC1-AT, the NMR frequency of ^{31}P shifted upfield ($\Delta\delta = -0.61$ and -1.13 ppm for the inner (P0) and outer (P1) phosphorus, respectively). Thus, the closest environments of P0 and P1 atoms became shielded. This observation permitted to conclude that the interaction of $HCrO_4^-$ ions with GC1-AT particles occurred mainly in the adjacent environment of P atoms of GC1 dendrimers. This interaction was likely responsible for the observed expansion of the interlayer space.

Because of the interaction of hydrochromate ions with CG2-AT particles, a slight shield ($\Delta\delta = -0.15$ ppm) of the environment of Si took place. Moreover, the environment of the inner atoms of P (P0) of the dendrimers was shielded ($\Delta\delta = -1.13$ ppm) (Table 6). Thus, the adsorption of $HCrO_4^-$ by CG2-AT happened at the level of the tetrahedral sheet as well as at the inner part of the retained CG2 dendrimers.

4. Conclusion

The results of the study of interactions between montmorillonite and phosphorus-based dendrimers enabled us to conclude that: (i) the main quantity of the compensating charge (Na^+) was expelled as a result of the adsorption of dendrimers. (ii) Dendrimers of the first generation were placed within the interlayer space and induced an appreciable expansion. In this case, intercalated nanocomposites were formed. (iii) The adsorption of the second generation of dendrimers resulted in the formation of exfoliated and intercalated nanocomposites. The confined dendrimers were strongly compressed.

The results of the studies of the adsorption of chromate on the nanocomposites and the Na-saturated montmorillonite showed that: (i) the kinetics process was mainly controlled by internal diffusion. (ii) The Temkin model fairly described the adsorption isotherms, and adsorption seemed to occur by chemisorption ($38 < \Delta H^\circ < 94$ kJ/mol). (iii) The maximum uptake amounts of the hexavalent chromium (6–10 mg/g) were higher than those reported for some organo-modified montmorillonite adsorbents. (iv) Chromate adsorption by Na-AT particles happened at the level of the silanol groups of the tetrahedral sheet of montmorillonite. For GC1-AT, it essentially occurred near the inner phosphorus of the dendrimers. In the case of CG2-AT, it took place at the tetrahedral sheet as well as at the core of the dendrimers.

Acknowledgments

The authors gratefully thank CNRS (France), CNRST (Morocco), EGIDE (France), and the LIA LCMMF for their financial support. They also thank Prof. Jean-Jacques Bonnet for administrative facilities.

Abbreviations

A	—	constant in the H-J adsorption model $(mmol/g)^2$
B	—	constant in the D-R adsorption model $(mol/J)^2$
B	—	constant in the Temkin adsorption model (J/mol)
B'	—	constant in the H-J adsorption model
C_e	—	equilibrium concentration of chromate in solution (mmol/L)
K_F	—	Freundlich constant
K_L	—	Langmuir constant (L/mol)
K_T	—	Temkin constant (L/mmol)
Q_e	—	adsorbed amount at equilibrium (mmol/g)
Q_m	—	adsorption capacity (mmol/g)
$1/n$	—	constant in the Freundlich adsorption model

References

[1] S. Komarneni, Feature article. Nanocomposites, J. Mater. Chem. 2 (1992) 1219–1230.
[2] A. Okada, A. Usuki, Twenty years of polymer-clay nanocomposites, Macromol. Mater. Eng. 291 (2006) 1449–1476.
[3] S. Yariv, H. Cross, Organo-Clay Complexes and Interactions, Marcel Dekker, New York, NY, 2002.
[4] F. Bergaya, B.K.G. Theng, G. Lagaly, Handbook of Clay Science. Development in Clay Science, vol. 1, Elsevier, Amsterdam, 2006.
[5] M. Alexandre, P. Dubois, Polymer-layered silicate nanocomposites: Preparation, properties and uses of a new class of materials, Mater. Sci. Eng. R: Report 28 (1–2) (2000) 1–63.

[6] S.S. Ray, M. Okamoto, Polymer/layered silicate nanocomposites: A review from preparation to processing, Prog. Polym. Sci. 28 (2003) 1539–1641.
[7] J.J. Decker, S.N. Chvalun, S. Nazarenko, Intercalation behavior of hydroxylated dendritic polyesters in polymer clay nanocomposites prepared from aqueous solution, Polymer 52 (2011) 3943–3955.
[8] A.S. Costa, T. Imae, Morphological investigation of hybrid Langmuir−Blodgett films of arachidic acid with a hydrotalcite/dendrimer nanocomposite, Langmuir 20 (2004) 8865–8869.
[9] T.Y. Juang, Y.C. Chen, C.C. Dai, S.A. Tsai, T.M. Wu, R.J. Jeng, Nanoscale organic/inorganic hybrids based on self-organized dendritic macromolecules on montmorillonites, Appl. Clay Sci. 48 (2011) 103–110.
[10] Q. Wang, J.L. Mynar, M. Yoshida, E. Lee, M. Lee, K. Okuro, K. Kinbara, T. Aida, High-water-content mouldable hydrogels by mixing clay and a dendritic molecular binder, Nature 463 (2010) 339–343.
[11] B. Sarkar, Y. Xi, M. Megharaj, G.S.R. Krishnamurti, D. Rajarathnam, R. Naidu, Remediation of hexavalent chromium through adsorption by bentonite based Arquad® 2HT-75 organoclays, J. Hazard. Mater. 183 (2010) 87–97.
[12] D. Mohan, C.U. Pittman Jr., Activated carbons and low cost adsorbents for remediation of tri- and hexavalent chromium from water, J. Hazard. Mater. 137 (2006) 762–811.
[13] C.H. Weng, Y.C. Sharma, S.H. Chu, Adsorption of Cr(VI) from aqueous solutions by spent activated clay, J. Hazard. Mater. 155 (2008) 65–75.
[14] K.Z. Setshedi, M. Bhaumik, S. Songwane, M.S. Onyango, Exfoliated polypyrrole-organically modified montmorillonite clay nanocomposite as a potential adsorbent for Cr(VI) removal, Chem. Eng. J. 222 (2013) 186–197.
[15] M. Hajjaji, H. El Arfaoui, Adsorption of methylene blue and zinc ions on raw and acid-activated bentonite from Morocco, Appl. Clay Sci. 46 (2009) 418–421.
[16] N. Launay, A.M. Caminade, J.P. Majoral, Synthesis of bowl-shaped dendrimers from generation 1 to generation 8, J. Organomet. Chem. 529 (1997) 51–58.
[17] C. Loup, M.-A. Zanta, A.-M. Caminade, J.P. Majoral, B. Meunier, Preparation of water-soluble cationic phosphorus-containing dendrimers as DNA transfecting agents, Chem.-A Eur. J. 5 (1999) 3644–3650.
[18] C. Padié, M. Maszewska, K. Majchrzak, B. Nawrot, A.M. Caminade, J.P. Majoral, Polycationic phosphorus dendrimers: Synthesis, characterization, study of cytotoxicity, complexation of DNA, and transfection experiments, New J. Chem. 33 (2009) 318–326.
[19] J. Basset, R.C. Denny, G.H. Jeffery, J. Mendham, Vogel's Textbook of Quantitative Inorganic Analysis, ELBS/Longman, London, 1986.
[20] Z. Sun, Y. Park, S. Zheng, G.A. Ayoko, R.L. Frost, XRD, TEM, and thermal analysis of Arizona Ca-montmorillonites modified with didodecyldimethylammonium bromide, J. Colloid Interface Sci. 408 (2013) 75–81.
[21] T. Holtzapffel, Les minéraux argileux: Préparation, analyse diffractométrique et détermination (Clay minerals: Preparation, analysis by X-ray diffraction, and identification), Société Géologique du Nord, vol. 12, I.S.S.N. 0291-3062, Villeneuve d'Asq, France, 1985.
[22] S. Komarneni, C.A. Fyfe, G.J. Kennedy, Detection of nonequivalent Si sites in sepiolite and palygorskite by solid-state 29Si magic angle spinning-nuclear magnetic resonance, Clays Clay Miner. 34 (1986) 99–102.
[23] D.E. Woessner, Characterization of clay minerals by 27Al nuclear magnetic resonance spectroscopy, Am. Mineral. 74 (1989) 203–215.
[24] Y. Sağ, Y. Aktay, Mass transfer and equilibrium studies for the sorption of chromium ions onto chitin, Proc. Biochem. 36 (2000) 157–173.
[25] H. Qiu, L. Lv, B.-C. Pan, Q.-J. Zhang, W.-M. Zhang, Q.-X. Zhang, Critical review in adsorption kinetic models, J. Zhejiang Univ. Sci. A 10(5) (2009) 716–724.
[26] O. Ferrandon, H. Bouabane, M. Mazet, Tests for the validity of different models used for the adsorption of solutes on activated carbon, Revue des sciences de l'eau 8 (1995) 183–200.
[27] C.H. Shiau, C.C. Pan, Adsorption of basic dyes from aqueous solution by various adsorbents, Sep. Sci. Technol. 39 (2004) 1733–1750.
[28] B.S. Krishna, D.S.R. Murty, B.S. Jai Prakash, Thermodynamics of chromium(VI) anionic species sorption onto surfactant-modified montmorillonite clay, J. Colloid Interface Sci. 229(1) (2000) 230–236.
[29] C. Weng, Y.C. Sharma, S. Chu, Adsorption of Cr(VI) from aqueous solutions by spent activated clay, J. Hazard. Mater. 155 (2008) 65–75.
[30] B.J. Hu, H.J. Luo, Adsorption of hexavalent chromium onto montmorillonite modified with hydroxyaluminum and cetyltrimethylammonium bromide, Appl. Surf. Sci. 257 (2010) 769–775.
[31] S.A. Khan, R. Riaz-ur-Rehman, M.A. Khan, Adsorption of chromium(III), chromium(VI) and silver(I) on bentonite, Waste Manage. 15 (1995) 271–282.
[32] B. Hu, H. Luo, H. Chen, Adsorption of chromate and para-nitrochlorobenzene on inorganic–organic montmorillonite, Appl. Clay Sci. 51 (2011) 198–201.
[33] M. Barkat, S. Chegrouche, A. Mellah, B. Bensmain, D. Nibou, M. Boufatit, Application of Algerian bentonite in the removal of cadmium(II) and chromium (VI) from aqueous solutions, J. Surf. Eng. Mater. Adv. Technol. 4 (2014) 210–226.
[34] S.T. Akar, Y. Yetimoglu, T. Gedikbey, Removal of chromium(VI) ions from aqueous solutions by using Turkish montmorillonite clay: effect of activation and modification, Desalination 244 (2009) 97–108.
[35] M. Eloussaief, N. Kallel, A. Yaacoubi, M. Benzina, Mineralogical identification, spectroscopic characterization, and potential environmental use of natural clay materials on chromate removal from aqueous solutions, Chem. Eng. J. 168 (2011) 1024–1031.
[36] E. Lippmaa, M. Maegi, A. Samoson, G. Engelhardt, A. Grimmer, Structural studies of silicates by solid-state high-resolution silicon-29 NMR, J. Am. Chem. Soc. 102 (1980) 4889–4893.